Enzyme and Microbial Technology 170 (2023) 110293

Contents lists available at ScienceDirect

Enzyme and Microbial Technology

journal homepage: www.elsevier.com/locate/enzmictec

Enzymatic functionalization of liquid phase exfoliated graphene using horseradish peroxidase and laccase

Aleksandra Mitrović [a,*], Jelena Milovanović [b], Jacek Gurgul [c], Andrijana Žekić [d], Jasmina Nikodinović-Runić [b], Veselin Maslak [a]

[a] University of Belgrade, Faculty of Chemistry, Studentski trg 16, P. O. B. 51, 11158 Belgrade, Serbia
[b] Institute of Molecular Genetics and Genetic Engineering, University of Belgrade, Vojvode Stepe 444a, 11221 Belgrade, Serbia
[c] Jerzy Haber Institute of Catalysis and Surface Chemistry, Polish Academy of Sciences, Niezapominajek 8, PL-30239 Kraków, Poland
[d] University of Belgrade, Faculty of Physics, Studentski trg 12, 11000 Belgrade, Serbia

ARTICLE INFO

Keywords:
Graphene
Graphene oxide
Biocatlysis
Enzymatic functionalyzation

ABSTRACT

We present a novel approach for the enzymatic functionalization of graphene, utilizing horseradish peroxidase (HPO) and laccase (LC) from *Trametes versicolor*. This study demonstrates, for the first time, the covalent modification of non-homogeneous graphene with a low surface-to-volume ratio, both in solution and on solid support. Through thermogravimetry analysis, we estimate the degree of functionalization to be 11% with HPO and 4% with LC, attributed to the varying redox potentials of the enzymes. This work highlights the potential of enzymatic reactions for tailored functionalization of graphene under mild conditions.

1. Introduction

Graphene, a two-dimensional (2D) material derived from graphite, has gained significant attention for its exceptional thermal and electrical conductivity, optical transparency, and mechanical properties [1–3]. These properties have led to the development of graphene-based electronics and photovoltaic systems [4,5]. However, despite its impressive physics, graphene's chemical reactivity is limited due to its inert nature, consisting of sp^2 hybridized carbon atoms with a large delocalized electron system. The environmental fate of graphene, especially its degradation and interactions with biomolecules, has become a subject scholarly of interest. Recent studies have demonstrated the capability of selected fungi and enzymes, such as human myeloperoxidase and eosinophil peroxidase, to degrade few-layer graphene into oxidized graphene (GO) [6–8]. The oxidation process introduces various oxygen-containing groups, making GO highly reactive for diverse chemical reactions. Additionally, GO can be easily dispersed in aqueous media and further degraded by neutrophils, eosinophil peroxidase, and horseradish peroxidase, leading to non-genotoxic products [9–11].

However, most of these biotransformations have been observed primarily for graphene sheets, which are generally considered low-dimensional or zero-dimensional (0D). Limited evidence exists for other biological transformations of graphene [12–14]. The growing number of studies focusing on the biodegradation of graphene and similar materials highlights the need for further investigation [15–17].

In general, enzymatic covalent functionalization of graphene involves using enzymes to catalyze reactions that result in the attachment of molecules onto the graphene surface. This can be achieved through enzymatic oxidation, where enzymes introduce reactive groups on the graphene surface, or enzymatic bioconjugation, where enzymes facilitate coupling reactions between functional groups on biomolecules and the graphene surface. The enzyme-mediated oxidation generates reactive species, such as radicals or peroxides, which can react with the functional groups on both the graphene surface and the biomolecule. This leads to the formation of covalent bonds, anchoring the molecules onto the graphene surface These approaches offer specificity, efficiency, and mild reaction conditions for precise and controlled functionalization resulting in materials with great potential [18–21].

In this study, our main objective was to explore the functionalization of non-homogeneous graphene in solution using oxidizing enzymes, specifically horseradish peroxidase (HPO) and laccase (LC). These enzymes have demonstrated effectiveness in oxidizing other carbon-rich materials [11,22,23]. We specifically chose non-homogeneous graphene samples, which consist of a mixture of graphene sheets with varying lateral sizes and thicknesses, to examine their behavior during the functionalization.

* Corresponding author.
E-mail address: afemic@chem.bg.ac.rs (A. Mitrović).

https://doi.org/10.1016/j.enzmictec.2023.110293
Received 7 April 2023; Received in revised form 19 July 2023; Accepted 20 July 2023
Available online 27 July 2023

By investigating enzymatic functionalization, this study aims to contribute to our understanding of their potential applications and the feasibility of controlled derivatization using enzymes. The results obtained from this work can pave the way for new avenues in the covalent functionalization of graphene and broaden its range of applications in various fields.

2. Experimental section

2.1. Materials and methods

SGN18 graphite was purchased from Future Carbon in Germany. Enzymes, 2,2′-azino-bis(3-ethylbenzothiazoline-6-sulfonic acid (ABTS), Dimethyl sulfoxide (DMSO), H_2O_2, and other solvents were bought from Sigma Aldrich and used as received. Horseradish peroxidase and Laccase (*Trametes versicolor laccase*) were purchased from Sigma in Munich, Germany, both in powder form.

Liquid phase exfoliation was conducted using an Ultrasonic bath, specifically the Bandelin Sonorex Super RK 52.

Raman Spectroscopy: Raman spectra were acquired using a LabRam HR Evolution confocal Raman microscope from Horiba. The microscope was equipped with an automated XYZ stage and 0.80 NA objectives. An excitation wavelength of 532 nm was primarily used for characterizing the covalently functionalized G. To enhance spectral resolution, a grating with 1800 grooves/mm was selected. The acquisition time for the spectra was 2 s unless stated otherwise. Additionally, the laser intensity was kept below 5% (0.88 mW) to prevent photo-induced laser oxidation of the samples.

Thermogravimetric analysis coupled to Mass Spectrometry: Thermogravimetric analysis was performed using a Netzsch STA 409CD Skimmer equipped with an EI ion source and a quadrupole mass spectrometer. The temperature profile was set to increase from 25° to 600°C at a ramp rate of 10 K/min, followed by cooling to 30 °C. The initial sample weights were adjusted to 5.0 (± 0.1) mg, and the entire experiment was conducted under an inert gas atmosphere with a helium (He) gas flow of 80 mL/min.

UV-Vis spectra were recorded using a COLO NOVEL4S UV–Vis spectrophotometer.

IR spectra (ATR) were obtained using a Perkin-Elmer FT-IR 1725X spectrophotometer. The ν values are reported in cm^{-1}.

Investigations of sample morphology were conducted using *scanning electron microscopy (SEM)* with a JEOL JSM-840A instrument equipped with an INCA Penta FETx3 EDX microanalyzer. The investigated samples were gold sputtered in a JFC 1100 ion sputterer before being subjected to SEM observations.

X-ray Photoelectron Spectroscopy (XPS) measurements were carried out using SES R4000 hemispherical analyzer (Gammadata Scienta, Sweden). Non-monochromatized AlK_α radiation (1486.6 eV) was used to generate core excitations. The X-ray tube was operated at 12 kV and an emission current of 15 mA. The energy resolution of the system, measured as the full width at half maximum (FWHM) for the Ag $3d_{5/2}$ line, was 0.9 eV (pass energy 100 eV). The spectrometer was calibrated according to ISO 15472:2001. The base pressure in the analytical chamber was 1×10^{-10} mbar and about 3×10^{-9} mbar during the experiments.

Powder samples were pressed into indium foil and mounted on a special holder inside the multi-chamber UHV system. The sample analysis area was about 4 mm^2 (5 ×0.8 mm). High-resolution spectra were collected at a pass energy of 100 eV (with 25 meV step), whereas survey scans were collected at a pass energy of 200 eV (with 0.25 eV step). The XPS spectra were registered at an incidence angle of 90° (to the sample surface).

Intensities were estimated by calculating the integral of each peak (in CasaXPS 2.3.23 software), after subtraction of the Shirley-type background and fitting the experimental curve with a pseudo-Voigt profile (combination of Gaussian and Lorentzian lines) of variable proportions (70:30). The samples were conductive, so all binding energy values are as obtained.

2.2. Synthetic procedures

Graphite SNG-18 was suspended in DMSO (2 mg/mL) and sonicated for 20 h. The suspension was then centrifuged at 5000 rpm for 10 min to remove the bulk material. The resulting dispersion was used for further enzymatic oxidations.

2.2.1. Preparation of Si/SiO_2 wafers

Graphite was suspended in isopropanol (1 mg/mL) and sonicated for 24 h. The suspension was then centrifuged at 5000 rpm for 10 min to remove the bulk material, and the supernatant was drop-casted onto Si/SiO_2 wafers (50 μL on each). The wafers were placed in a 24-well plate, and reactions were initiated in each well by adding the appropriate buffer, mediator, and enzyme.

2.2.2. Horseradish peroxidase assay

2.2.2.1. On Si/SiO_2 wafers. The wafers with the graphene layer were placed in a 24-well plate. The reaction was set up in triplicate, with the addition of 190 μL of phosphate buffer (50 mM, pH 6), 300 μL of 0.5% H_2O_2, and 10 μL of a fresh cold suspension of HPO (10 mg/mL) in phosphate buffer (50 mM, pH 6) to each well. The plate was then incubated at 30 °C with shaking at 70 rpm for 14 days. On days 7 and 10, a fresh cold solution of HPO (5 μL, concentration 10 mg/mL) and 150 μL of 0.5% H_2O_2 were added to each well.

A control reaction was set up in the same manner, but without the enzyme, and another control was prepared with the wafer in phosphate buffer. After 14 days, the silicon wafers were thoroughly washed with water/ethyl acetate, and the remaining material was further analyzed.

2.2.2.2. In solution. The graphene solution in DMSO (7.5 mL) was diluted with 142.5 mL of phosphate buffer (50 mM, pH 6) and sonicated for 20 min to obtain a solution with a graphene concentration of approximately 0.1 mg/mL.

The reaction was initiated with 75 mL of this stock solution by adding 3 mL of 0.5% H_2O_2 and 1 mL of a fresh cold suspension of horseradish peroxidase (HPO) (10 mg/mL) in phosphate buffer (50 mM, pH 6). The mixture was then incubated at 30 °C with shaking at 180 rpm for 14 days. On days 7 and 10, a fresh solution of HPO (0.5 mL, concentration 10 mg/mL) and 1.5 mL of 0.5% H_2O_2 were added.

A control reaction was set up in the same manner but without the enzyme HPO. Another control was prepared with graphene in phosphate buffer. After 14 days, the product was obtained by centrifugation and subjected to a thorough workup with water.

2.2.3. Laccase assay

2.2.3.1. On Si/SiO_2 wafers. The wafers with a graphene layer were placed in a 24-well plate. The reaction was set up in triplicate, with the addition of 480 μL of acetate buffer (50 mM, pH 4.5), 10 μL of ABTS (concentration 0.1 mg/mL in 50 mM acetate buffer, pH 4.5), and 10 μL of a fresh cold suspension of laccase (20 mg/mL) in acetate buffer (50 mM, pH 4.5) to each well. The plate was then incubated at 37 °C with shaking at 70 rpm for 14 days. On days 7 and 10, a fresh cold solution of laccase (5 μL, concentration 20 mg/mL) and 5 μL of ABTS (concentration 0.1 mg/mL, same buffer) were added to each well. A control reaction was set up in the same manner but without the enzyme. Another control was prepared with the wafer in acetate buffer. After 14 days, the silicon wafers were thoroughly washed with water/ethyl acetate, and the remaining material was further analyzed.

2.2.3.2. In solution. The graphene solution in DMSO (7.5 mL) was

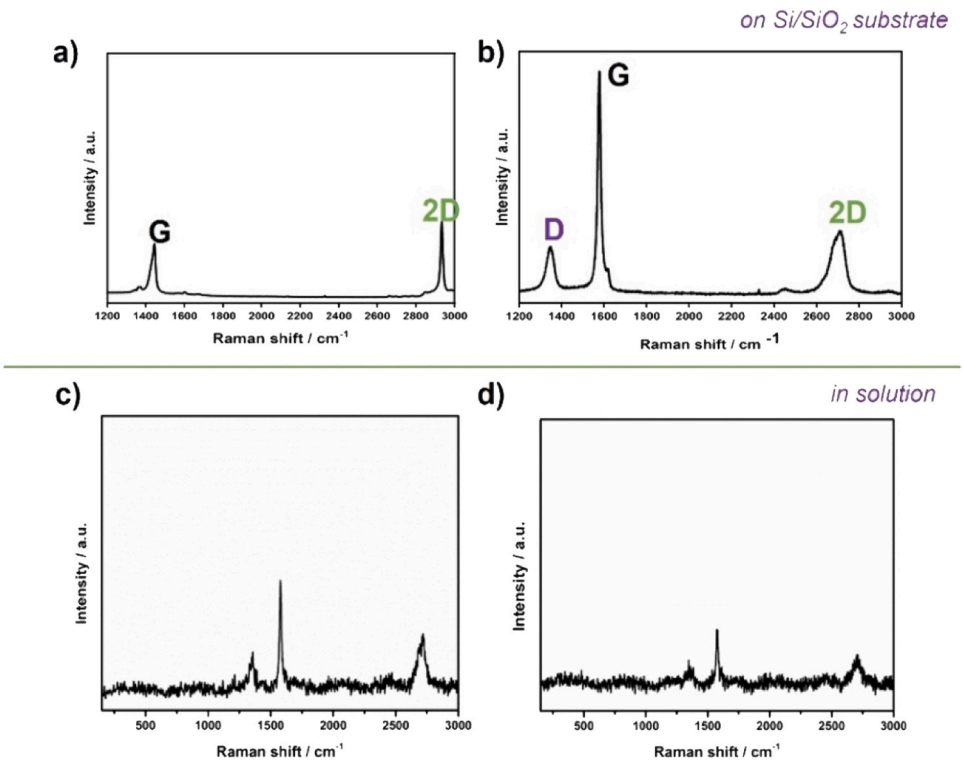

Fig. 1. a) Raman spectra of bulk graphite, b) Average Raman mean spectra of the sample flake treated with HPO enzyme (112 data points) on Si/SiO_2 wafer. Mean Raman spectra of c) HPO-treated sample d) LC-treated sample in solution. For the Raman spectra of the control samples, refer to Supporting Information, Figs. S1–2.

diluted with 142.5 mL of acetate buffer (50 mM, pH 4.5) and sonicated for 20 min to obtain a solution with a graphene concentration of approximately 0.1 mg/mL.

The reaction was initiated with 60 mL of this stock solution by adding 100 μL of ABTS (concentration: 1 mg/mL in 50 mM acetate buffer, pH 4.5) and 1 mL of a fresh cold suspension of laccase (20 mg/mL) in acetate buffer (50 mM, pH 4.5). The mixture was then incubated at 37 °C with shaking at 180 rpm for 14 days. On days 7 and 10, additional laccase solution (0.5 mL, concentration: 20 mg/mL in acetate buffer 50 mM, pH 4.5) and 50 μL of ABTS (concentration: 1 mg/mL, same buffer) was added.

After 14 days, the product was obtained by centrifugation and subjected to thorough a workup with water.

3. Results and discussion

High-quality graphene on a large scale can be produced through the liquid phase exfoliation (LPE) of graphite in specific organic solvents [24]. During the LPE procedure, graphite is often exfoliated into plate-like graphene particles. These particles, due to their two-dimensional nature, tend to self-aggregate and form stacks or restack. Enzymes typically require direct contact with the active sites on the surface of the material to initiate functionalization reactions. However, when graphene sheets stack together, the active sites become buried within the interlayer regions, hindering enzyme accessibility [25]. Our first strategy aimed to address this problem by investigating whether enzymes could access and functionalize the active surface of graphene when it is deposited on Si/SiO_2 wafers. These wafers, which contained graphene on their surfaces, served as substrates for enzymatic reactions with HPO and LC. The reactions were conducted in the presence of appropriate mediators for 14 days at a mild temperature. The samples were subsequently analyzed using scanning Raman spectroscopy (SRM). For each selected flake, an individual Raman spectrum was collected for a given number of points and plotted as an average mean spectrum to afford a representative image of the functionalized graphene flake.

Fig. 1 illustrates a single-point spectrum of the initial graphite and the average Raman mean spectra of graphene treated with HPO. In the graphite spectrum, the primary in-plane vibrational modes G (1446 cm^{-1}) and 2D (2935 cm^{-1}) are prominent. However, the graphene sample treated with HPO exhibited a different in-plane vibration, specifically the D band at 1349 cm^{-1}, and G and 2D bands at 1578 cm^{-1} and 2715 cm^{-1}, respectively. The Raman mappings revealed defects in the graphene structure, similar to those obtained through microbial oxidation of graphene [26,27]. Although the intensity of the D band was not as strong as in chemically produced graphene oxide, it could still be attributed to the presence of functional groups attached to the graphene surface. Based on this observation, we were motivated to pursue a more extensive investigation into the functionalization of graphene through a wet chemistry approach on a larger scale, despite the inherent risks of restacking.

In order to conduct the functionalization experiments, we utilized an LPE method to exfoliate graphite, with DMSO serving as the solvent. DMSO was selected due to its compatibility with enzymes, tolerating its presence up to 30% v/v in usual activity assays [28,29]. However, we aimed to minimize the amount of organic solvent used, so we limited it to 5% v/v. The functionalization experiments were carried out in solution by combining HPO, LC, and appropriate mediators with DMSO graphene dispersions in phosphate/acetate buffer. The obtained reaction mixtures were stirred and maintained at 37 °C /30 °C for 14 days. Additionally, control experiments were performed by incubating graphene suspensions with H_2O_2/ABTS alone to evaluate any potential structural changes in the material. The amounts of enzymes used were adjusted according to the literature, for the HPO we referred to the oxidation of graphene oxide [11]. As for the functionalization of graphene with laccase, the procedure was guided by literature for the graphene-like material using [30], since graphene itself had not been employed in this manner before.

The resulting material was initially analyzed using Raman spectroscopy, and the mapping obtained for HPO/LC is presented in Fig. 1c,

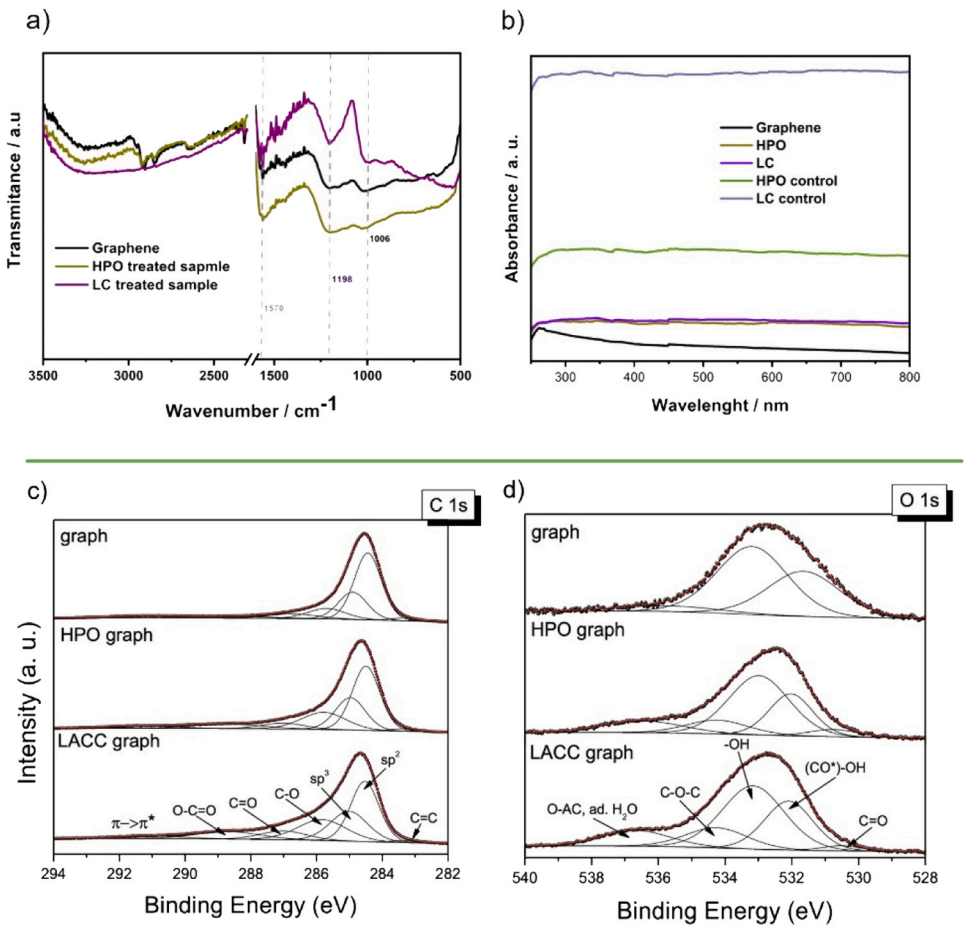

Fig. 2. a) ATR-FTIR spectra of pristine graphene, HPO/LC treated samples. Proposed assignments 1570 cm^{-1} and 2900 cm^{-1} are skeletal graphitic vibrations with adsorbed water. (For the full range spectra, please refer to Supporting Information, Fig. S3). b) UV–vis spectra of the enzyme treated material which was resuspended in isopropanol (IPA). c) High-resolution XPS spectra of C 1 s line of graphene, modified graphene. (HPO- and LC-treated samples). (d) High-resolution XPS spectra of O 1 s line of graphene, modified graphene (HPO- and LC-treated samples). The acronym ``O-AC`` stands for O atoms bonded to the aromatic carbon.

d. It is important to note that the samples were mapped as powder, utilizing low laser power and short acquisition times to prevent lattice destruction. Consequently, the collected signals exhibited lower intensity levels. The average spectrum obtained aligns well with previously obtained spectra from reactions on solid supports, displaying the presence of a D band at 1358 cm^{-1}.

In the study, vibrational absorption spectroscopy was utilized to investigate the prepared material, focusing on the observation of vibrational modes associated with COOH, C–OH, C–H, and C═O functionalities (Fig. 2a). However, when compared to graphene, no distinct features are observable in the HPO-treated sample. Interestingly, in the case of laccase functionalization, a well-defined band attributed to the C-OH stretch (1198 cm^{-1}) is observed, indicating the presence of hydrogen bonds around 3000 cm^{-1}. Notably, absorption peaks in the UV–vis spectrum were only observed in graphene at 265 nm. The absence of distinct bands in the treated material could be a result of low functionalization, but it is also strongly influenced by the size and concentration of the flakes (Fig. 2b) [31,32].

In the XPS spectra, distinctive peaks corresponding to carbon (C 1 s) and oxygen (O 1 s) were observed (Fig. 2c, d). The C 1 s spectra of the initial material and the enzyme-treated sample exhibited similar shapes, but a closer quantitative analysis revealed variations in the contributions of different components. Deconvolution of the C 1 s peak enabled the identification of various carbon functional groups, including C-C, C-O, and C═O, indicating oxidation and the presence of oxygen-containing groups. On the other hand, the shapes of the O 1 s spectra exhibited significant differences among themselves (Fig. 2d). The presence of oxygen functionalities, including hydroxyl (-OH), carbonyl (C═O), and epoxy (C-O-C) groups, was detected, suggesting the persistence of remnants from the graphene oxide structure even in

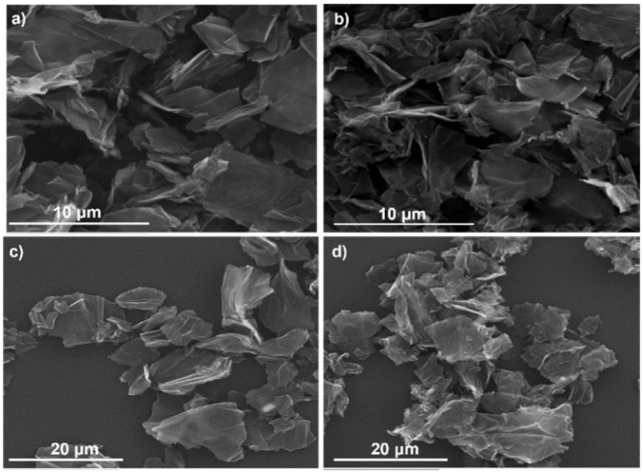

Fig. 3. SEM images of the samples treated with a) HPO, b) LC, c) LC- control, d) HPO - control.

graphene itself, possibly due to prolonged sonication times. Furthermore, the laccase-functionalized samples exhibited a higher contribution of epoxy and aromatic O-C bonds compared to graphene (quantitatively 14% of C-O-C vs. O% and 12% of O-AC/ad·H_2O vs. 7%, respectively).

Scanning electron microscopy (SEM) was conducted to examine the morphological changes of the graphene samples following incubation with HPO and LC. The obtained SEM images revealed a layered sheet structure of the material, with no apparent differences observed

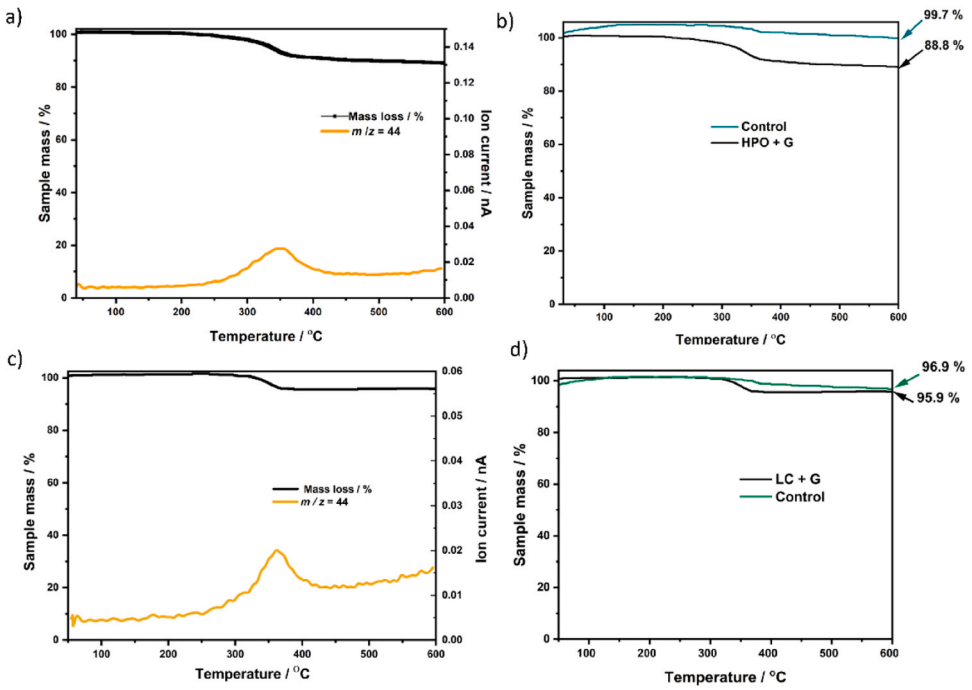

Fig. 4. a) TGA/MS characterization of the product treated HPO enzyme. b) d) Comparison of the TGA profiles between enzyme treated sample and the control one. c) TGA/MS characterization of the product treated with LC. Complete TGA profiles with full range of ion currents are for clarity reasons moved to Supporting Information, see Fig S4-7.

between the enzyme-treated samples and the control samples (Fig. 3). In the energy-dispersive X-ray (EDX) analysis of the same material, only the presence of oxygen could be detected in selected areas of the enzyme-treated samples, without a definitive confirmation of its fraction (refer to Supporting Information, Fig. S8-9).

To evaluate the accurate degree of functionalization of graphene, we employed thermogravimetric analysis (TGA) coupled with mass spectroscopy (MS), which involved increasing the temperature under an inert atmosphere. Fig. 4a illustrates the TGA/MS analysis of the graphene sample treated with horseradish peroxidase (HPO) enzyme. The sample was heated to 600 °C, and the released gases were analyzed using mass spectrometry. The primary weight loss step was observed around 330 °C, corresponding to the evolution of CO and CO_2 gases. In contrast, the TGA analysis of the control sample exhibited thermally stable behavior with no significant change in mass. Thus, it can be inferred that the approximate 11% mass loss in the treated sample resulted from the functionalization of graphene (Fig. 4a). In the case of the laccase-treated material, TGA analysis revealed a weight loss of only 4%, while the control sample exhibited a 3% mass loss (Fig. 4d). This indicates that no significant functionalization occurred with the laccase enzyme. This outcome is expected due to the lower redox potential of laccase compared to peroxidase enzymes [33]. The conclusion that HPO is a better oxidant than laccase is consistent with the published redox potentials for these enzymes. In addition, the redox potential of peroxidase intermediates and free radicals generated during enzymatic catalysis plays a very important role in the oxidation process [17]. Hayashi and Yamasaki [34] determined redox potentials of ~950 mV for HRP compound I/compound II and compound 1I/ferric couples at slightly acidic pH values. For laccase from *T. versicolor*, Reinhammar [35] determined redox potentials of 785 and 782 mV for the Type 1 and Type 3 copper sites, respectively.

A comparison with the control samples allowed us to distinguish between functionalization and physically adsorbed molecules that might remain trapped between the layers of graphene, despite the thorough preparation and drying process. One characteristic of trapped reagents or solvent molecules in thermogravimetric analysis (TGA) is their low detachment temperature, typically below 100 °C. However, our samples exhibited high detachment temperatures, indicating the presence of chemically functionalized groups that are thermally stable. The main weight loss in both cases occurred around 350 °C and is likely attributed to the C-OH bonds. It is also possible for weight loss to occur if the mediators oxidize the material.

TG analysis revealed that graphene functionalization did not occur with H_2O_2 alone, without the enzyme. These findings are consistent with previous reports indicating that oxidation to graphene oxide (GO) does not occur solely with H_2O_2 treatment, highlighting the crucial role of the enzyme [36]. However, when using ABTS alone, a 3% formation of autoxidized material was observed. XPS analysis further confirmed the presence of oxidized forms of graphene in the control sample which consisted of 24% of C═O, 36% of COOH, 11% of C-O-C bond, and 29% of O-AC/adsorbed water. (see Fig S10 in Supporting Information). While the overall percentage of oxidized material is relatively low, this observation is significant and has previously only been reported with azulene [37].

4. Conclusion

In conclusion, our investigation into the enzymatic functionalization of graphene revealed the presence of functional groups attached to the graphene surface. The enzymatic reactions led to observable shifts in Raman peaks and the detection of oxygen in selected areas. Thermogravimetric analysis coupled with mass spectroscopy indicated the evolution of CO and CO_2 gases, confirming the presence of thermally stable oxidative groups resulting from functionalization. Comparisons with control samples further supported the conclusion that the weight loss observed in the treated samples was due to functionalization rather than physically adsorbed molecules. These findings provide valuable insights into the enzymatic modification of non-homogeneous and realistic forms of graphene, which closely resemble the samples used in the production of carbon-based nanomaterials. Overall, enzymatic functionalization offers advantages in terms of mild reaction conditions, environmental friendliness, versatility, compatibility with biological

systems, and potential for greener synthesis. These advantages make enzymatic approaches attractive for functionalizing materials like graphene, opening up opportunities for tailored modifications with controlled properties and enhanced functionality.

CRediT authorship contribution statement

Aleksandra Mitrović: Conceptualization, Investigation, Funding acquisition, Writing – original draft, Writing – review & editing. Jelena Milovanović: Conceptualization, Investigation, Writing – review & editing, Jacek Gurgul: XPS analysis. Andrijana Žekić: Collecting SEM and EDX data. Jasmina NIkodinović – Runić: Writing – review & editing, Supervision. Veselin Maslak: Writing – review & editing, Supervision.

Data availability

Data will be made available on request.

Acknowledgments

This work was supported by PMI/Centre for Leadership Belgrade through the "Start-up for Science" program. We would also like to acknowledge the Alexander von Humboldt Foundation for granting A. M. a renewed stay in Germany. We are grateful to Professor Andreas Hirsch for providing access to the Raman spectrometer and TGA/MS.

Conflicts of interest

We declare no competing financial interests.

Appendix A. Supporting information

Supplementary data associated with this article can be found in the online version at doi:10.1016/j.enzmictec.2023.110293.

References

[1] K.S. Novoselov, A.K. Geim, S.V. Morozov, D. Jiang, Y. Zhang, S.V. Dubonos, I. V. Grigorieva, A.A. Firsov, Electric field effect in atomically thin carbon films, Science 306 (5696) (2004) 666–669.
[2] A.A. Balandin, S. Ghosh, W. Bao, I. Calizo, D. Teweldebrhan, F. Miao, C.N. Lau, Superior thermal conductivity of single-layer graphene, Nano Lett. 8 (3) (2008) 902–907.
[3] C. Lee, X. Wei, J.W. Kysar, J. Hone, Measurement of the elastic properties and intrinsic strength of monolayer graphene, Science 321 (5887) (2008) 385–388.
[4] E.P. Randviir, D.A.C. Brownson, C.E. Banks, A decade of graphene research: production, applications and outlook, Mater. Today 17 (9) (2014) 426–432.
[5] M.D. Stoller, S. Park, Y. Zhu, J. An, R.S. Ruoff, Graphene-based ultracapacitors, Nano Lett. 8 (10) (2008) 3498–3502.
[6] C. Martín, G. Jun, R. Schurhammer, G. Reina, P. Chen, A. Bianco, C. Ménard-Moyon, Enzymatic degradation of graphene quantum dots by human peroxidases, Small 15 (52) (2019), 1905405.
[7] R. Kurapati, S.P. Mukherjee, C. Martín, G. Bepete, E. Vázquez, A. Pénicaud, B. Fadeel, A. Bianco, Degradation of single-layer and few-layer graphene by neutrophil myeloperoxidase, Angew. Chem. Int Ed. Engl. 57 (36) (2018) 11722–11727.
[8] C. Martín, K. Kostarelos, M. Prato, A. Bianco, Biocompatibility and biodegradability of 2D materials: graphene and beyond, Chem. Commun. 55 (39) (2019) 5540–5546.
[9] S.P. Mukherjee, A.R. Gliga, B. Lazzaretto, B. Brandner, M. Fielden, C. Vogt, L. Newman, A.F. Rodrigues, W. Shao, P.M. Fournier, M.S. Toprak, A. Star, K. Kostarelos, K. Bhattacharya, B. Fadeel, Graphene oxide is degraded by neutrophils and the degradation products are non-genotoxic, Nanoscale 10 (3) (2018) 1180–1188.
[10] R. Kurapati, C. Martìn, V. Palermo, Y. Nishina, A. Bianco, Biodegradation of graphene materials catalyzed by human eosinophil peroxidase, Faraday Discuss. 227 (2021) 189–203.
[11] G.P. Kotchey, B.L. Allen, H. Vedala, N. Yanamala, A.A. Kapralov, Y.Y. Tyurina, J. Klein-Seetharaman, V.E. Kagan, A. Star, The enzymatic oxidation of graphene oxide, ACS Nano 5 (3) (2011) 2098–2108.
[12] J. Zhao, Z. Wang, J.C. White, B. Xing, Graphene in the aquatic environment: adsorption, dispersion, toxicity and transformation, Environ. Sci. Technol. 48 (17) (2014) 9995–10009.
[13] M. Pelin, S. Sosa, M. Prato, A. Tubaro, Occupational exposure to graphene based nanomaterials: risk assessment, Nanoscale 10 (34) (2018) 15894–15903.
[14] I. Sorrentino, I. Stanzione, Y. Nedellec, A. Piscitelli, P. Giardina, A. Le Goff, From graphite to laccase biofunctionalized few-layer graphene: a “one pot” approach using a chimeric enzyme, Int. J. Mol. Sci. 21 (11) (2020) 3741.
[15] M. Chen, X. Qin, G. Zeng, Biodegradation of carbon nanotubes, graphene, and their derivatives, Trends Biotechnol. 35 (9) (2017) 836–846.
[16] R. Kurapati, C. Martìn, V. Palermo, Y. Nishina, A. Bianco, Biodegradation of graphene materials catalyzed by human eosinophil peroxidase, Faraday Discuss. 227 (0) (2021) 189–203.
[17] G.P. Kotchey, S.A. Hasan, A.A. Kapralov, S.H. Ha, K. Kim, A.A. Shvedova, V. E. Kagan, A. Star, A natural vanishing act: the enzyme-catalyzed degradation of carbon nanomaterials, Acc. Chem. Res. 45 (10) (2012) 1770–1781.
[18] M. Daniyal, B. Liu, W. Wang, Comprehensive review on graphene oxide for use in drug delivery system, Curr. Med Chem. 27 (22) (2020) 3665–3685.
[19] G. Yildiz, M. Bolton-Warberg, F. Awaja, Graphene and graphene oxide for bio-sensing: General properties and the effects of graphene ripples, Acta Biomater. 131 (2021) 62–79.
[20] C. Chung, Y.-K. Kim, D. Shin, S.-R. Ryoo, B.H. Hong, D.-H. Min, Biomedical applications of graphene and graphene oxide, Acc. Chem. Res. 46 (10) (2013) 2211–2224.
[21] S. Han, J. Sun, S. He, M. Tang, R. Chai, The application of graphene-based biomaterials in biomedicine, Am. J. Transl. Res 11 (6) (2019) 3246–3260.
[22] I. Gitsov, A. Simonyan, L. Wang, A. Krastanov, S.W. Tanenbaum, D. Kiemle, Polymer-assisted biocatalysis: Unprecedented enzymatic oxidation of fullerene in aqueous medium, J. Polym. Sci. Part A Polym. Chem. 50 (1) (2012) 119–126.
[23] G.P. Kotchey, Y. Zhao, V.E. Kagan, A. Star, Peroxidase-mediated biodegradation of carbon nanotubes in vitro and in vivo, Adv. Drug Deliv. Rev. 65 (15) (2013) 1921–1932.
[24] Y. Xu, H. Cao, Y. Xue, B. Li, W. Cai, Liquid-phase exfoliation of graphene: an overview on exfoliation media, techniques, and challenges, Nanomaterials 8 (11) (2018).
[25] V.C. Sanchez, A. Jachak, R.H. Hurt, A.B. Kane, Biological interactions of graphene-family nanomaterials: an interdisciplinary review, Chem. Res Toxicol. 25 (1) (2012) 15–34.
[26] A. Kaniyoor, S. Ramaprabhu, A Raman spectroscopic investigation of graphite oxide derived graphene, AIP Adv. 2 (3) (2012), 032183.
[27] C. Zhu, Q. Hao, Y. Huang, J. Yang, D. Sun, Microbial oxidation of dispersed graphite by nitrifying bacteria 2011.2, Nanoscale 5 (19) (2013) 8982–8985.
[28] M.-H. Wu, M.-C. Lin, C.-C. Lee, S.-M. Yu, A.H.J. Wang, T.-H.D. Ho, Enhancement of laccase activity by pre-incubation with organic solvents, Sci. Rep. 9 (1) (2019) 9754.
[29] A.M. Azevedo, D.M.F. Prazeres, J.M.S. Cabral, Ls.P. Fonseca, Stability of free and immobilised peroxidase in aqueous–organic solvents mixtures, J. Mol. Catal. B Enzym. 15 (4) (2001) 147–153.
[30] C. Zhang, W. Chen, P.J.J. Alvarez, Manganese peroxidase degrades pristine but not surface-oxidized (carboxylated) single-walled carbon nanotubes, Environ. Sci. Technol. 48 (14) (2014) 7918–7923.
[31] T. Zhang, G.-Y. Zhu, C.-H. Yu, Y. Xie, M.-Y. Xia, B.-Y. Lu, X. Fei, Q. Peng, The UV absorption of graphene oxide is size-dependent: possible calibration pitfalls, Microchim. Acta 186 (3) (2019) 207.
[32] S.E. Bourdo, R. Al Faouri, R. Sleezer, Z.A. Nima, A. Lafont, B.P. Chhetri, M. Benamara, B. Martin, G.J. Salamo, A.S. Biris, Physicochemical characteristics of pristine and functionalized graphene, J. Appl. Toxicol. 37 (11) (2017) 1288–1296.
[33] P.J. Kersten, B. Kalyanaraman, K.E. Hammel, B. Reinhammar, T.K. Kirk, Comparison of lignin peroxidase, horseradish peroxidase and laccase in the oxidation of methoxybenzenes, Biochem. J. 268 (2) (1990) 475–480.
[34] Y. Hayashi, I.J.Jobc Yamazaki, The oxidation-reduction potentials of compound I/ compound II and compound II/ferric couples of horseradish peroxidases A2 and C, 254(18) (1979) 9101–9106.
[35] B. R. M. Reinhammar, Oxidation-reduction potentials of the electron acceptors in laccases and stellacyanin 275 (2) (1972) 245–259.
[36] R. Kurapati, C. Martín Jiménez, V. Palermo, Y. Nisina, A. Bianco, Biodegradation of graphene materials catalyzed by eosinophil peroxidase from human immune cells, Faraday Discuss. 227 (2020).
[37] M.A. Pickard, R. Roman, R. Tinoco, R. Vazquez-Duhalt, Polycyclic aromatic hydrocarbon metabolism by white rot fungi and oxidation by coriolopsis gallica UAMH 8260 laccase, Appl. Environ. Microbiol. 65 (9) (1999) 3805–3809.